Chapter 3

A Nested Slot and T-Match Network Based Hybrid Antenna for UHF RFID Tag Applications

3.1 Introduction

In recent past years, Radio Frequency Identification (RFID) technique has been reaching its heights in the area of Agriculture, EPS (Electronic Payment Systems), Access control, Libraries, Marathons, Hospitals and many more resourceful applications[37]. RFID systems operate on four different frequency bands[38] , with specific allocations varying by country or region[39], as discussed in Section 2.3.

RFID tags in UHF band are most needed in today's commercial world. UHF RFID tags are smaller in size compared to LF and HF tags along with less multipath interference. They provide higher read range albeit low transmitting power. In UHF RFID tag, backscatter modulation technique is used, in which the reader antenna sends EM wave as interrogator to the tag. The UHF tag happens to be nothing but a transducer which converts this incoming interrogator into electrical signal. The UHF tag comprises a semiconductor microchip namely ASIC(Application Specific Integrated Circuit), which is used for

input impedance matching[40]. Input impedance of RFID microchip is capacitive in nature and impedance matching is done with inductive impedance of the UHF tag antenna. Impedance matching techniques in UHF RFID tag design and miniaturization of size was explained in [41]. The complex conjugate impedance matching in UHF RFID tag is actualized by conjoining either of T-match network, inductively coupled loop or nested slot. In T-match method, the input impedance of the dipole is altered by using short circuit stub. T-match network summate inductive element to the antenna input impedance so that it can be able to compensate the capacitive impedance of the microchip.

Matching in T-match network is acquired by altering the length and width of the branches. [42], describes how a T-match tag antenna matched with NXP UCODE G2X IC having impedance $24 - j163\ \Omega$ at 875 MHz. In [43], T-Match network introduced in form of loop to match the SRR(Split-Ring Resonator) UHF tag antenna. [44] demonstrates a T-match network for impedance matching with NXP UCODE G2XM microchip with its equivalent circuit analysis and reported a peak read range value of 11 meters at 898 MHz.

Nesting configurations in antenna design for RFID tag have been developing as a prominent contender. This configuration provides multiband, extensive bandwidth[45], complex impedance matching[46] characteristics along with contraction of antenna size[47]. Nested slot based impedance matching is applicable for larger planar dipoles having higher permittivity substrate. In this method, the total slot size is comparable to the patch area. A nested slot configuration in RFID tag, used for remote healthcare operations is introduced in [48]. The article used to match the tag with impedance of Impinj R6 microchip. Although by using nested slot in patch, mediocre impedance matching was obtained. The maximum read range of the antenna obtained was only 3 meters although tag had very small size.

It is realized from above literature that impedance matching with microchip is a foremost task for RFID tag design. For this purpose, in previous literatures, three methods i.e., T-match, Inductive coupled loop or Nested slot have been used. In this proposed work, a combination of three techniques i.e., meandered line, T-match and Nested slot have been used to get commendable complex conjugate impedance matching. Thus hybridization

of aforementioned techniques produces a novel RFID tag antenna in UHF India band. It is realized that this designed antenna has adequate measured read range in contrast with earlier designs. The tag complex impedance,impedance matching with IC Alien Higgs-4 SOT, reflection coefficient and read range have been presented.

3.2 UHF Tag Design

The geometric shematic of the tendered antenna for UHF RFID tag is shown in Figure 3.1. The tag has trace of $120mm \times 60mm \times 1.6mm$ built on Rogers RT/duroid 5880 substrate (ϵ_r=2.2, tanδ=0.0009) having thickness of 1.6 mm. This antenna is designed inside a nested slot. The tag antenna is consisting a symmetric T-match network in the nested slot providing conjugate impedance matching with the microchip. The most available microchips namely ASIC's have the resistance upto few tenfold while the capacitive reactance is found to be upto few centuple. The semiconductor microchip used in this RFID UHF tag antenna is Alien Higgs-4 SOT[5], which is having the sensitivity of -18.5 dBm during the reading mechanism. The microchip have the complex input impedance of $20.5 - j191.2\Omega$ at 865 MHz. The result clarifies the simulated 10 dB-return loss bandwidth obtained of the proposed tag antenna is 12 MHz (859 MHz-871 MHz).

Design Methodology and Initial Parameters: To achieve a compact design, a mean-

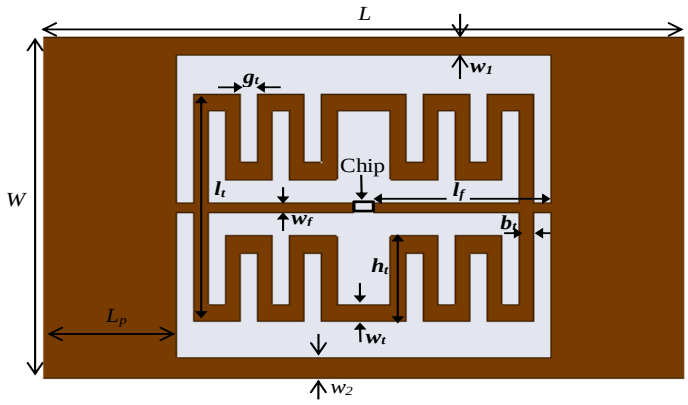

Figure 3.1: Schematic of the tendered antenna

dering structure was employed to reduce the overall size of the antenna, while impedance

matching was addressed using a nested slot and a symmetric T-match network. These features were incorporated in the initial geometry to target resonance near 865 MHz. The nested slot structure was adopted to induce inductive reactance, matching the highly capacitive chip impedance (20.5 - j191.26 Ω). The starting dimensions for the T-match loop and slot were based on standard transmission line theory and prior designs reported in the literature[41, 49]. Iterative simulations were conducted to vary parameters like the T-strip width (w_t), length (l_t), and the frame width (w_f) to fine-tune impedance matching. The optimized dimensions, as listed in Table 3.1, were finalized when the simulated impedance closely approached the conjugate of the chip impedance.

The resonance frequency is tuned by altering the dimensions of the nested slot, feed line and introducing T-match and thus matching the tag impedance with the chip is achieved. The optimum values of geometrical parameters of the proposed antenna to obtain the impedance matching is shown in Table 3.1. Initially, Nested slot is imposed in the patch

Table 3.1: Optimized Values Of Geometrical Parameters Of The Tag Antenna

Parameters	Values(mm)	Parameters	Values(mm)
L	120	b_t	3
W	60	L_p	25
w_t	3	w_f	1.5
l_f	33	w_1	3
g_t	3	w_2	3.5
l_t	40	h_t	15

and impedance matching between the antenna and microchip is observed. Due to not perfectly matching with microchip, a T-match network with meander lines is introduced in the nested slot. The steps to achieve the impedance matching with microchip is shown in figure 3.2. The overall substrate size ($L \times W$), nested slot area and the feed length and width remain same in all steps. The further effects of nested slot, meandered T-match network and symmetric end structure on various characteristics are now investigated. For the UHF tag antenna design, a nested slot is used for impedance matching as shown in Figure 3.2(a), and this structure resonates at 845 MHz. In Figure 3.2(b), the one side nested slot is superimposed by meandered T-matching network, hence, enabling the tag antenna to resonate at 854 MHz. The inductance of the meandered T-match network can be expressed

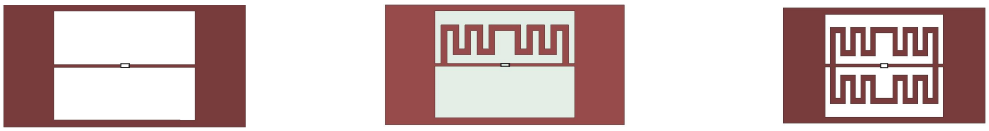

(a)Antenna I (b)Antenna II (c)Antenna III

Figure 3.2: Transformation steps of proposed antenna, (a) UHF Tag with Nested slot, (b) UHF tag with sigle sided T-match network inside Nested slot, (c) UHF tag with double-sided symmetric T-match network inside Nested slot.

as[50]:

$$L = 0.2l\left[\ln\left(\frac{l}{w+t}\right) + 1.19 + 0.022\left(\frac{w+t}{l}\right)\right] nH/mm \tag{3.1}$$

where l is total meandered T-match network length in mm, t is thickness in mm and w is width in mm. Here, total length of meandered T-match network, $l = 97mm$. The thickness(t) and periodic width(w) are 3mm and 6mm respectively.

Figure 3.2(c) presents the final structure of tag antenna with symmetric T-match meandered network inside nested slot. The symmetric T-match introduces parallel inductance resulting in reduced effective inductance and proposed antenna resonates at the desired frequency of 865 MHz. The simulated impedance matching and reflection coefficient of all the three cases are shown in figure 3.3.

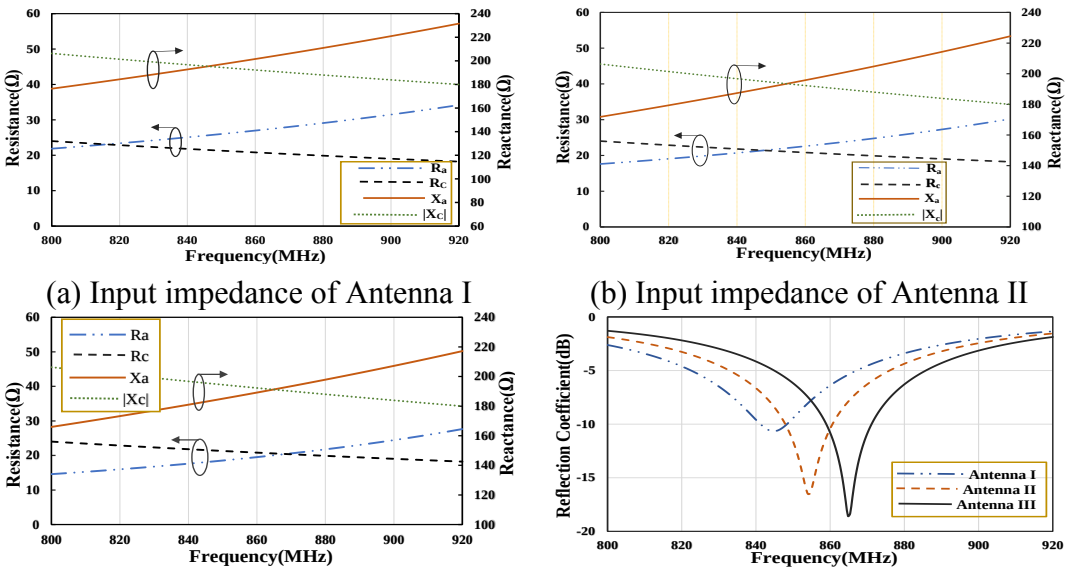

(a) Input impedance of Antenna I (b) Input impedance of Antenna II

(c) Input impedance of Antenna III (d) Simulated reflection coefficient

Figure 3.3: Simulated impedance matching and reflection coefficient of every step. R_a and X_a are resistance and inductive reactance of tag antenna respectively. R_c and $|X_c|$ represents resistance and absolute value of capacitive reactance of microchip respectively.

The first case i.e. tag antenna with nested slot is referred as Antenna I and its impedance matching graph is shown in Figure 3.3(a). The second case i.e. tag antenna with single sided T-match meandered network inside the nested slot is referred as Antenna II and its impedance matching graph is shown in Figure 3.3(b). The final structure i.e. tag antenna with double-sided symmetric T-match network inside nested slot is reffered as Antenna III and its impedance matching graph is shown in Figure 3.3(c). The simulated reflection coefficient graph of all the three antennas is shown in Figure 3.3(d).

For proper functioning of the RFID tag, the tag input impedance should be matched to chip impedance for maximum power transfer. The microchip switches its input impedance in two states i.e. shorted state & matched state.When the microchip is matched to tag, the incoming signal from reader is absorbed by the transducer and chip changes to short state. In short state, the interrogator signal is retransmitted to the reader. The obtained impedance of the tag at 865 MHz is $20 + j191.2\Omega$. The return loss is calculated by the given formula in Eq. 3.2:

$$\Gamma = \frac{Z_c - Z_a^*}{Z_c + Z_a} \tag{3.2}$$

where Z_c and Z_a are microchip and tag antenna input impedance respectively, where Z_a= $R_a + jX_a$ and $Z_c = R_c + jX_c$, where X_c is negative.

The tag antenna consists of a radiating body and the T-match rectangular loop, which are inductively coupled. After combining radiating body and the T-match loop, the two terminals are attached to the microchip. The strength of coupling is controlled by loop-gap, shape of the T-match loop and the strip width. The equivalent circuit of the rectangular T-matching loop antenna is shown in Figure 3.4. The tag antenna input impedance is given by [51]

$$Z_a = R_a + jX_a = Z_{Tm} + \frac{(2\pi f M)^2}{Z_r} \tag{3.3}$$

where Z_r and Z_{TM} are the impedances of radiating body and T-match loop respectively.

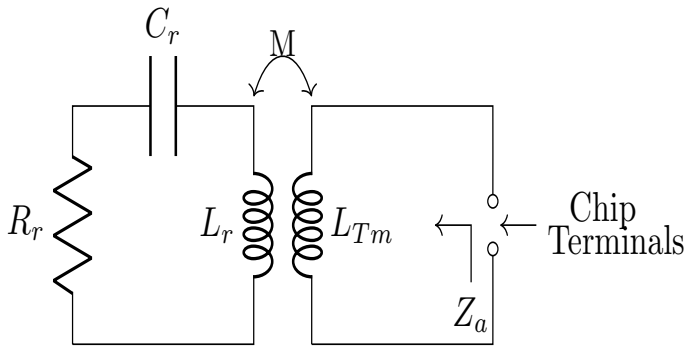

Figure 3.4: Inductively coupled T-match loop equivalent circuit

M is mutual inductance between the inductances. Z_r is calculated by:

$$Z_r = R_{r,0} + jR_{r,0}Q_r\left(\frac{f}{f_0} - \frac{f_0}{f}\right) \tag{3.4a}$$

where, $R_{r,0}$ is resistance of the radiating body at resonance frequency, Q_r is the quality factor and f_0 is resonating frequency. Impedance of T-match network can be calculated by:

$$Z_{Tm} = j2\pi f L_{Tm} \tag{3.4b}$$

The resistance and reactance at resonating frequency can be calculated by:

$$R_a\left(f = f_0\right) = \frac{\left(2\pi f_0 M\right)^2}{R_{r,0}} \tag{3.5a}$$

$$X_a\left(f = f_0\right) = 2\pi f_0 L_{Tm} \tag{3.5b}$$

where L_{Tm} is the inductance of meandered T-match network which is obtained from equation 3.1. Thus, by using above equations, the real and imaginary part of the tag antenna impedance is obtained which is plotted in Figure 3.3(c).

3.3 Parametric Analysis

Every geometrical parameter has different effect on input impedance and reflection coefficient of the tendered antenna. Parametric analysis is being carried out by altering one

parameter at a time and keeping other parameters constant. The impact of variation of meandered T-match network width(w_t), feed line width(w_f), length of T-match network (l_t) on impedance matchning and return loss is investigated. Variation of w_t and l_t elaborates effect of T-match network on impedance matching and w_f elaborates effect of varying nested slot area on impedance matching.

In order to analyze the response of these parameters on input impedance and return loss, the tag antenna is simulated by varying parameter w_t from 2mm to 4mm while keeping other parameters constant. It is realized from Figure 3.5(a) that real part of impedance matching increases with increase in w_t. When w_t is 2mm, we find the real part of impedance is matched on 836.7 MHz while imaginary part matches with the semiconductor chip reactance on 854.2 MHz. Thus the difference between matching is 17 MHz and tag antenna resonates at 853 MHz with poor return loss having 8 MHz 10-dB return loss bandwidth.

For $w_t = 3mm$, it is observed antenna resonates at 865 MHz with 12 mHz 10-dB return

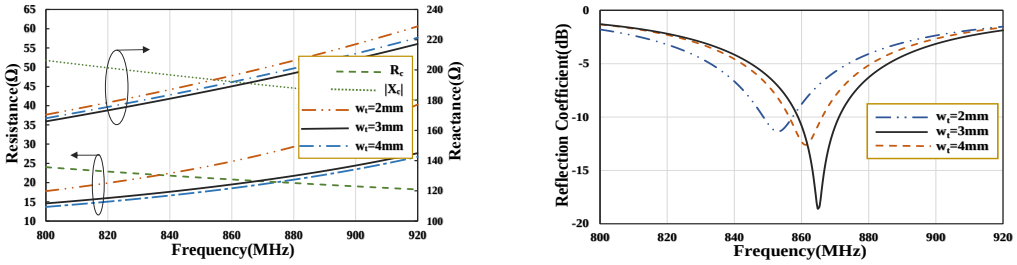

(a) (b)

Figure 3.5: (a) Simulated input impedance and (b) Reflection Coefficient for different values of w_t.

loss bandwidth.When $w_t = 4mm$, real part of tag antenna matches with microchip resistance at 875 MHz while reactance matches at 860 MHz. At this value the difference is 15 MHz and antenna resonates at 861.2 MHz with 9.6 MHz 10-dB return loss bandwidth. The reflection coefficient for these values of w_t is shown in Figure 3.5(b). Thus, the value of w_t for optimum reflection coefficient is found to be 3mm.

To investigate the effect of l_t on performance of tag antenna, it is varied from 38mm to 42mm while keeping other parameters constant. From Figure 3.6, it is realized that we find optimum return loss for $l_t = 40mm$.

For $l_t = 38mm$, the real part of input impedance tag matches with microchip resistance at

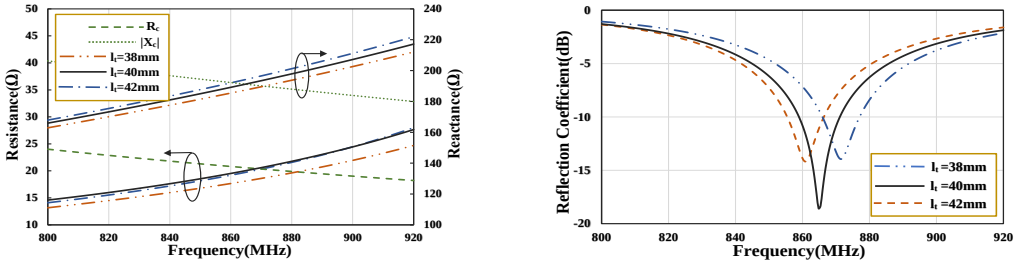

(a) (b)

Figure 3.6: (a) Simulated input Impedance and (b) Reflection Coefficient for different values of l_t.

881.8MHz and imaginary part is matched at 871 MHz.Thus, there is 10.8 MHz frequency gap between matching.For this value, tag antenna resonates at 871.4 MHz with 10.8 MHz 10-dB return loss bandwidth. Further, resonating frequency reduces with increasing l_t. For $l_t = 42mm$, real part of tag antenna matches with microchip resistance at 870 MHz and imaginary part matches with microchip reactance at 860 MHz, thus frequency separation between matching is 10 MHz. Hence tag antenna resonates at 860.6 MHz with poor return loss having 10.2 MHz 10-dB return loss bandwidth.

Figure 3.7(a) depicts the simulated resistance and reactance of input impedance of proposed structure with different values of w_f, ranging from 1mm to 2mm, keeping other parameters unaltered. For $w_f = 1mm$, the real part of tag and microchip impedance are

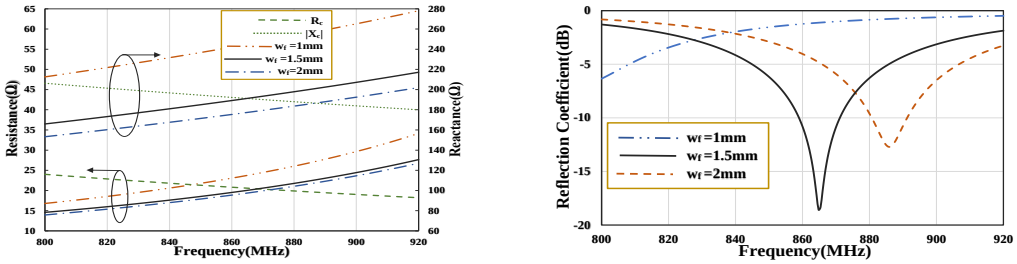

(a) (b)

Figure 3.7: (a) Simulated input impedance and (b) Reflection Coefficient for different values of w_f.

equal at 847 MHz, while the imaginary part matches below the UHF band for RFID tags. Further, increasing the value of w_f, complex impedance matching is achieved at 865 MHz for $w_f = 1.5mm$. Increasing the value of w_f results in higher resonating frequency. For $w_f = 2mm$, the real part equals to microchip resistance at 872.8MHz and imaginary part

of tag antenna matches with reactance of microchip at 886.8 MHz. Thus it is observed there is 14 MHz gap. Tag antenna resonates at 885.8 MHz with 10 MHz 10-dB return loss bandwidth. The return loss for these feed line widths are shown in Figure 3.7(b). It is contemplated from the parametric study that with the optimized values of the aforementioned parameters, input impedance of UHF tag antenna is 20 + j191.2Ω at 865 MHz, which is almost the complex conjugate of the microchip impedance.

3.4 Results and Discussions

The fabricated prototype of the RFID tag antenna with Rogers RT/duroid 5880 substrate is shown in Figure 3.8. As the proposed antenna structure is a balanced structure, hence, the input impedance and reflection loss cannot be measured by using simply single ended two-port Vector Network Analyser. If a balanced tag antenna is connected to an unbal-

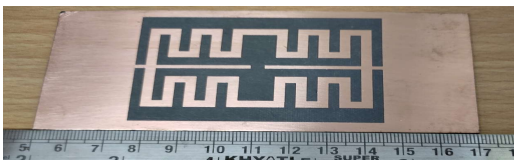

Figure 3.8: Fabricated prototype of proposed RFID tag antenna

Figure 3.9: Semi-rigid differential probe used for impedance measurement

anced port, then unequal current flows in the tag antenna. Thus accurate measurement of impedance of the balanced tag antenna becomes tough. Hence, authors used differential probe method[52] based input impedance measurement which is shown in Figure 3.9 with Anritsu MS2038C VNA. The measurement setup of impedance using differential probe is shown in Figure 3.10. One end of the differential probe is connected to the VNA with cables and other end, which has small exended inner conductors, is connected to antenna under test as shown in figure 3.11.

The S-parameters of the proposed antenna are measured by aforementioned VNA and then by using following conversion formula[53], the differential input impedance (Z_{diff})

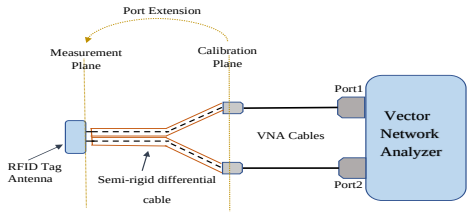

Figure 3.10: Measurement schematic setup with differential probe

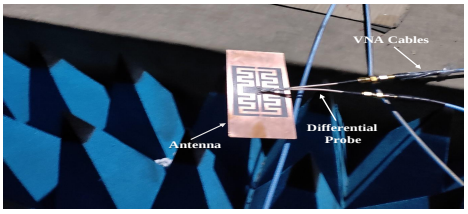

Figure 3.11: Impedance measurement of tag antenna

of the tag antenna is calculated.

$$Z_{diff} = \frac{2Z_0\left(1 - S_{11}S_{22} + S_{12}S_{21} - S_{12} - S_{21}\right)}{\left(1 - S_{11}\right)\left(1 - S_{22}\right) - S_{21}S_{12}} \tag{3.6}$$

Figures 3.12 and 3.13 show measured and simulated input impedance and reflection coefficient of the proposed antenna respectively. The measured input impedance is $20.9 + j191.2\Omega$ at 865 MHz, while the same achieved by simulation is $20 + j191.2\Omega$ which is approximate to complex conjugate of microchip impedance. The measured 10-dB reflection coefficient bandwidth is 9 MHz(861.5 MHz-870.5 MHz). The slight incongruity between the measured and simulation results can be attributed to port extension errors and fabrication imperfections.

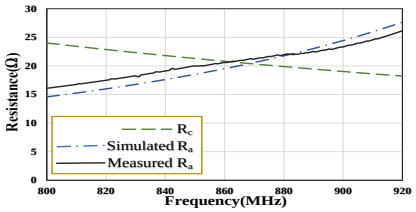

(a)Measured and simulated resistance.

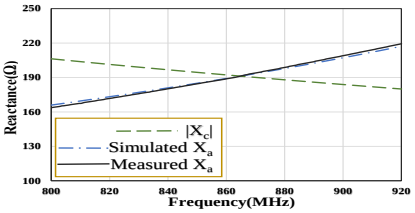

(b)Measured and simulated reactance.

Figure 3.12: Measured and simulated input impedance of proposed antenna

The maximum separation distance between the reader and tag for activation of chip is

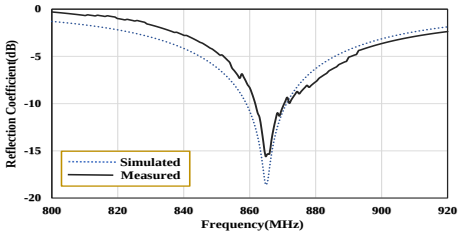

Figure 3.13: Measured and simulated reflection coefficient of RFID tag antenna.

given by Eq. 3.7.

$$S_{max}(\theta,\phi) = \frac{\lambda}{4\pi}\sqrt{\frac{EIRP_R}{P_{th,chip}}(1-|\Gamma|^2)G_t(\theta,\phi)} \tag{3.7}$$

where $G_t(\theta,\phi)$ is the gain of tag antenna and $(1-|\Gamma|^2)$ is efficiency due to impedance mismatches. The tag is tested for 4W EIRP reader and the microchip sensitivity, $P_{th,chip}$= -18.5 dBm.

The $G_t(\theta,\phi)$ is expressed as [54],

$$G_t(\theta,\phi) = \tau\eta_{cd}D \tag{3.8}$$

where,

$$\tau = (1-|\Gamma|^2) \tag{3.9}$$

is impedance mismatch efficiency, η_{cd} is the efficiency as a result of dielectric and conductor losses i.e. radiation efficiency. The simulated realized gain of every transformation step is shown in Figure 3.14. Gain of the proposed antenna is over -0.52 dBi covering -10dB bandwidth. The measured and simulated maximum separation between tag and reader, which is the read range, is sketched in figure 3.15. Table 3.2 testifies a compar-

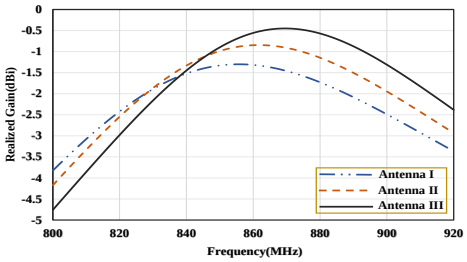

Figure 3.14: Simulated gain of the tag antenna at the boresight.

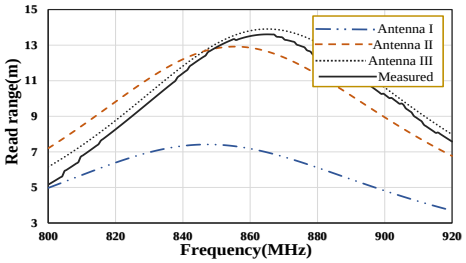

Figure 3.15: Measured Read range obtained of the proposed tag antenna.

ison among this work and other erstwhile reported antennas in similar band in terms of chip used, substrate, dimensions and read range.The comparison is done for those UHF tags which are operated in the same vicinity of frequency of operation as of the proposed antenna. The semiconductor microchip used in the proposed work has lowest sensitivity to provide better tag-reader separation. In the proposed antenna, authors have used different

Table 3.2: Various parameters comparison of the tendered antenna with few previous reported antenna

Antenna	Microchip	Sensitivity (dBm)	Substrate	Dimensions (mm^3)	Frequency (MHz)	Gain (dBi)	Read range(m)
[55]	Higg-2	-17	FR4	$100 \times 60 \times 10$	870	$--$	12.2
[56]	Higgs-2	-15	FR4	$120 \times 30 \times 1.5$	868	$--$	3.5
[57]	IC of $Z_{in} = 22-j195\Omega$	-15	GML 1000	$105 \times 60 \times 0.76$	866	$--$	7.3
[58]	Monza4	-17.4	RO4350B	$18 \times 4 \times 2$	867	$--$	3
[16]	Higgs-3	-18	FR4	$26 \times 8 \times 1.55$	867	-13	2.8
[59]	Higgs-4	-18.5	Copper-clad alumina	$23 \times 23 \times 1$	866	-17	1.2
[60]	Monza 5	-17.8	PP4 foam	$31.5 \times 31.5 \times 3.2$	867	-5.35	7.25
Proposed work	Higgs-4 SOT	-18.5	RT/duroid 5880(tm)	$120 \times 60 \times 1.6$	865	-0.47	13.9

substrate compared to other works . It can be seen that the gain achieved is much higher than most of the antennas. However, the proposed antenna size has larger dimensions but it provides far more tag-reader separation distance.

3.5 Outcome

In this article, a novel hybrid T-matched network is produced inside a nested slot. The antenna is matched to Alien Higgs-4 microchip for the maximum power transfer. Parametric analysis of the proposed structure is done. The obtained 10 dB return loss bandwidth is found to be 12 MHz i.e. RFID tag antenna is operatable in the range of 859 MHz to 871 MHz. The equivalent circuit of the proposed antenna is explained to make it easier to examine the working principle of the tag.As a result, an enhanced separation distance is obtained. This tag antenna spreads its tag to reader separation upto 13.9 meters, which makes it applicable to automatic vehicle identifying applications.

The detailed examination of the Nested Slot and T-Match Network in Chapter 3 offers insight into efficient impedance matching for UHF RFID tags operating at around 865 MHz. Moving into Chapter 4, we introduce the Meandered Inductive Loop structure, which addresses size reduction without compromising impedance matching. This

approach is particularly relevant for tags requiring compact designs while still maintaining sufficient read range. By operating at 866 MHz, the antenna design in this chapter further enhances compatibility with compact UHF RFID systems, making it well-suited for space-constrained applications like luggage tracking.